

Augmented Binary Substitution: Single-pass CDR germ-lining and stabilization of therapeutic antibodies

Sue Townsend^a, Brian J. Fennell^a, James R. Apgar^b, Matthew Lambert^a, Barry McDonnell^a, Joanne Grant^a, Jason Wade^a, Edward Franklin^a, Niall Foy^a, Deirdre Ní Shúilleabháin^a, Conor Fields^a, Alfredo Darmanin-Sheehan^a, Amy King^b, Janet E. Paulsen^b, Timothy P. Hickling^c, Lioudmila Tchistiakova^b, Orla Cunningham^a, and William J. J. Finlay^{a,1}

^aGlobal Biotherapeutics Technologies, Pfizer Biotherapeutics R&D, Dublin D22, Ireland; ^bGlobal Biotherapeutics Technologies, Pfizer Biotherapeutics R&D, Cambridge, MA 02139; and ^cPharmacokinetics, Dynamics and Metabolism, Pfizer Biotherapeutics R&D, Andover, MA 01810

Edited by Max D. Cooper, Emory University, Atlanta, GA, and approved October 27, 2015 (received for review June 4, 2015)

Although humanized antibodies have been highly successful in the clinic, all current humanization techniques have potential limitations, such as: reliance on rodent hosts, immunogenicity due to high non-germ-line amino acid content, v-domain destabilization, expression and formulation issues. This study presents a technology that generates stable, soluble, ultrahumanized antibodies via single-step complementarity-determining region (CDR) germ-lining. For three antibodies from three separate key immune host species, binary substitution CDR cassettes were inserted into preferred human frameworks to form libraries in which only the parental or human germ-line destination residue was encoded at each position. The CDR-H3 in each case was also augmented with 1 ± 1 random substitution per clone. Each library was then screened for clones with restored antigen binding capacity. Lead ultrahumanized clones demonstrated high stability, with affinity and specificity equivalent to, or better than, the parental IgG. Critically, this was mainly achieved on germ-line frameworks by simultaneously subtracting up to 19 redundant non-germ-line residues in the CDRs. This process significantly lowered non-germ-line sequence content, minimized immunogenicity risk in the final molecules and provided a heat map for the essential non-germ-line CDR residue content of each antibody. The ABS technology therefore fully optimizes the clinical potential of antibodies from rodents and alternative immune hosts, rendering them indistinguishable from fully human in a simple, single-pass process.

antibody | paratope | plasticity | humanization | immunogenicity

Monoclonal antibodies are a highly established technology in drug development and the majority of currently approved therapeutic antibodies are derived from immunized rodents (1). The advent of display libraries and engineered animals that can produce “fully human” antibody v-gene sequences has had a significant positive impact on antibody drug discovery success (1), but these technologies are mostly the domain of biopharmaceutical companies. Antibodies from wild-type animals that are already extant, or can be freely developed, will therefore continue to be a rich source of therapeutic candidates. In addition, phylogenetically distant hosts such as rabbits and chickens may become a valuable source of monoclonals with clinical potential against challenging targets (2, 3).

Chimerization of murine antibodies can reduce anti-IgG responses in man (4), but murine v-domains may still have provocative T-cell epitope content, necessitating “humanization” of their framework regions (5, 6). Classical humanization “grafts” murine CDRs into human v-gene sequences (7), but this typically leads to significant reduction in affinity for target, so murine residues are introduced at key positions in the frameworks (a.k.a. “back-mutations”), to restore function (8). Importantly, humanized antibodies do elicit lower immunogenicity rates in patients in comparison with chimerics (9).

Alternative humanization methods have also been developed based on rational design or empirical selection (10–17), but current methods still all suffer from flaws, such as: high non-germ-line

amino acid content retention (5, 6); grafting into poorly understood frameworks (13); resource-intensive, iterative methods (15, 18); requirement for homology modeling of the v-domains, which is often inaccurate (19, 20), or a cocrystal structure with the target antigen (14). Methods that allow humanization into preferred frameworks can add numerous framework mutations (18, 21), which may destabilize the v-domains (22), encode new T-cell epitopes, or introduce random amino acid mutations in CDRs (12, 13) that can drive polyspecificity and/or poor PK properties (23).

Critically, testing of protein therapeutics in monkeys has been shown to be nonpredictive of immune responses in man (24) and animal immunogenicity testing has been suggested to be of little value in biosimilar development (25). Current evidence suggests that the main risk factors for antibody immunogenicity in man are human T-cell epitope content and, to a lesser extent, T-cell independent B-cell responses (6). B-cell epitopes are challenging to predict and B-cell-only responses to biotherapeutics appear to be driven by protein aggregates (26). The key attributes to reduce antibody immunogenicity risk in the clinic appear to be: low T-cell epitope content, minimized non-germ-line amino acid content and low aggregation potential (27).

In recent years, several reports have strongly suggested that CDRs might be malleable in ways that could not be predicted a priori. Random mutagenesis and reselection of a classically humanized rat antibody found that individual framework back

Significance

Immunized animals are a key source of monoclonal antibodies used to treat human diseases. Before clinical use, animal antibodies are typically “humanized” by laborious and suboptimal methods that transfer their full target binding loops (a.k.a. CDRs) into human frameworks. We report an optimal method, where the CDRs from species such as rodents and chickens can be adapted to fit human frameworks in which we have clinical and manufacturing confidence. The Augmented Binary Substitution (ABS) process exploits the fundamental plasticity of antibody CDRs to ultrahumanize antibodies from key species in a single pass. ABS results in a final antibody that is much closer to human germ line in the frameworks and CDRs, minimizing immunogenicity risks in man and maximizing the therapeutic potential of the antibody.

Author contributions: S.T., L.T., and W.J.J.F. designed research; S.T., B.J.F., J.R.A., M.L., B.M., J.G., J.W., E.F., N.F., D.N.S., C.F., A.D.-S., A.K., J.E.P., T.P.H., O.C., and W.J.J.F. performed research; S.T., B.J.F., J.R.A., M.L., B.M., J.G., J.W., E.F., N.F., D.N.S., C.F., A.D.-S., A.K., J.E.P., T.P.H., O.C., and W.J.J.F. analyzed data; and S.T. and W.J.J.F. wrote the paper.

Conflict of interest statement: All authors are current or former employees of Pfizer.

This article is a PNAS Direct Submission.

Freely available online through the PNAS open access option.

¹To whom correspondence should be addressed. Email: william.finlay@pfizer.com.

This article contains supporting information online at www.pnas.org/lookup/suppl/doi:10.1073/pnas.1510944112/-DCSupplemental.

mutations and CDR residues could revert to human germ-line sequence, while maintaining or even improving the function of the antibody (28). A number of humanization studies have now also shown that a small number of positions in the CDRs could be substituted for human germ-line residues, through a rational design cycle of reversion mutations (5, 29). In addition to these observations, a number of structural analyses have illustrated the common redundancy of sequence space in antibody binding interfaces. Despite typically large buried interfaces between antibodies and protein targets, only a subset of residues in the CDRs of antibodies usually makes contact with antigen (30–32). Alanine scanning of CDR loops has also shown that only a limited number of residues directly affect antigen binding affinity (33). Indeed, it has even been shown that redundant paratope space in a single antibody may be exploited to engineer binding specificity to two separate targets (34). Additionally, CDR loop structures are known to be restricted to a limited number of canonical classes, despite amino acid variation within those classes at specific positions (35–38). These observations led us to hypothesize that, under the right experimental conditions, a large proportion of residues in grafted animal CDRs could be concurrently replaced by the residues found at the corresponding positions in a given destination human germ-line v-gene.

In this study, we generated combinatorial libraries on the basis of a design principle we have named “Augmented Binary Substitution” (ABS). Each library was based on a single starting antibody: rat anti-RAGE (28), rabbit anti-A33 (2), and chicken anti-pTau (3). These libraries were built into human germ-line frameworks of high predicted stability and solubility, then interrogated via phage display and screened to identify lead clones with epitope specificity and affinity equivalent to the parental clone. ABS proved to be a facile, rapid method that retains only the functionally required CDR content of the parental animal antibody, without the need for prior crystal-structure insight. Notably, this CDR germ-lining approach generated highly stable and soluble human IgGs, from multiple key antibody discovery species, that have minimized predicted human T-cell epitope content. The reproducibility of these findings across three antibodies from three disparate species demonstrates a fundamental plasticity in antibody paratopes that can be broadly exploited in therapeutic antibody optimization.

Results

Library Design, Build, and Characterization. Rat anti-RAGE XT-M4 (28), rabbit anti-A33 (2), and chicken anti-pTau pT231/pS235_1 (3) IgGs were generated on the human IgG1 backbone with either parental (Par-RAGE, Par-A33, or Par-pTau), grafted (Graft-RAGE, Graft-A33, or Graft-pTau), or classically humanized (CL-Hum-RAGE, CL-Hum-A33) v-domains. In scFv format, the parental form of each of these antibodies retained antigen binding, whereas the human FW-grafted versions demonstrated little to no binding (Fig. S1A–C). ABS ultrahumanization libraries (ABS-RAGE, ABS-A33, ABS-pTau) were constructed (Fig. 1) to generate 1.8×10^9 independent clones for ABS-RAGE, 1.1×10^{10} for ABS-A33, and 4.9×10^9 for ABS-pTau (theoretical binary diversity for ABS-RAGE is 2^{27} positions = 1.34×10^8 , for ABS-A33 $2^{32} = 4.29 \times 10^9$, and for ABS-pTau $2^{33} = 8.59 \times 10^9$). Library build quality was verified by sequencing ≥ 96 clones/library (Fig. S2). Libraries were rescued using helper phage M13 and selections performed on their cognate targets.

Identification and Analysis of Ultrahumanized clones. Postselection screening (Fig. S3A and B) and DNA sequencing revealed the presence of numerous scFv clones with significantly increased human content within the CDRs. In the ABS-RAGE and ABS-A33 leads, the FW sequences remained fully germ line. In the ABS-pTau leads ($n = 188$), all selected clones retained the T46 back-mutation (Kabat numbering used throughout), illustrating

that this VL-FW2 residue is essential to humanize chicken antibodies (Fig. S4). From each screen, ABS lead clones were ranked on the basis of HTRF signal vs. level of CDR germ-lining. The top 10 clones from each ranking were then subcloned into IgG expression vectors for further testing as below. Human germ-line amino acid content was quantified within the CDRs of parental antibodies and ABS leads and expressed as a percentage (Table S1). Human content had raised 17–29% in each case. In expression in HEK-293expi cells after transfection with IgG expression plasmids and expifectamine, all IgGs studies (ABS-derived leads and controls) produced >15 mg/L of purified IgG, with the exception of Graft-A33, which could not be expressed.

Lead IgG Affinity, Stability, and Specificity Characteristics. ABS leads in human IgG1 format were analyzed for specificity and stability. HTRF data (Fig. S5A–C), showed that the lead ABS-derived IgGs had successfully maintained full epitope competition with their respective parental clones (Table S1). Biacore analyses showed approximately twofold affinity improvements for C7-ABS-RAGE and C21-ABS-pTau over Par-RAGE and Par-pTau, respectively, whereas C6-ABS-A33 maintained equivalent affinity to Par-A33 (Table S1).

A baculovirus ELISA (Fig. S6A) where binding is a risk indicator for poor pK in vivo (39) showed no reactivity for any of the RAGE, A33, or pTau clones in comparison with an internal positive control (40). High-sensitivity Biacore assays were also established, to examine the possibility that v-gene engineering might lead to low-affinity interactions with multiple classes of proteins. A panel of 18 nontarget proteins showed that C7-ABS-RAGE and C6-ABS-A33 both maintained highly specific binding to their respective antigens (Fig. S6B and C). For the anti-pTau antibodies, specificity for pT231/pS235 was confirmed using previously described Biacore assays (3) (Fig. S6D). All ABS-derived leads in this study were, therefore, absent of the “charge asymmetry,” lipophilicity, off-target protein binding, or other problems that can arise during v-gene engineering (39, 41–43).

DSC analysis of IgG thermal stabilities demonstrated that C7-ABS-RAGE, C6-ABS-A33, and C21-ABS-pTau were highly stable. C7-ABS-RAGE was particularly thermostable with a Fab Tm of 85 °C; similar to Graft-RAGE, but almost 8 °C higher than that of the CL-Hum-RAGE (Fig. S7A and Table S1). This is a finding of note, as it highlighted that the presence of back-mutations in CL-Hum-RAGE had significantly decreased the stability of the v-domains in comparison with the highly stable graft. C21-ABS-pTau exhibited a Fab Tm of 70 °C, 4 °C higher than Graft-pTau (Fig. S7B). C6-ABS-A33 exhibited a Fab Tm of 74 °C, identical to Chim-A33 (Table S1), but could not be compared with Graft-A33, which could not be expressed at usable levels in our hands (Fig. S7C). In forced aggregation analyses, C7-ABS-RAGE, C21-ABS-pTau, and C6-ABS-A33 all showed $<10\%$ aggregation at 60 °C (Fig. S7D, E, F, Table S1). Graft-pTau, in contrast, exhibited $>90\%$ aggregation at 60 °C. Importantly, analysis of pH shock tolerance (which mimics virus-killing pH hold in mAb manufacturing) also showed each of the IgGs to be highly stable, with $<3\%$ loss observed (Table S1).

Human T-Cell Epitope Minimization in ABS Leads. ABS leads and associated precursors were examined for potential T-cell epitope content, as suggested in the recent FDA immunogenicity assessment guidelines (44), using the EpiMatrix software (6) for each clone (Fig. S8A). C7-ABS-RAGE, C6-ABS-A33 and C21-ABS-pTau showed scores of -53.72 , -50.22 , and -67.33 points, respectively. ABS lowered the projected immunogenicity of all clones into the same range as antibodies such as trastuzumab and lower than fully human antibodies such as adalimumab (Fig. S8A). Analysis at the individual peptide level predicted that T-cell epitope content was clearly reduced for all ABS leads in comparison with their respective parental forms (Fig. S9). Indeed, the removal

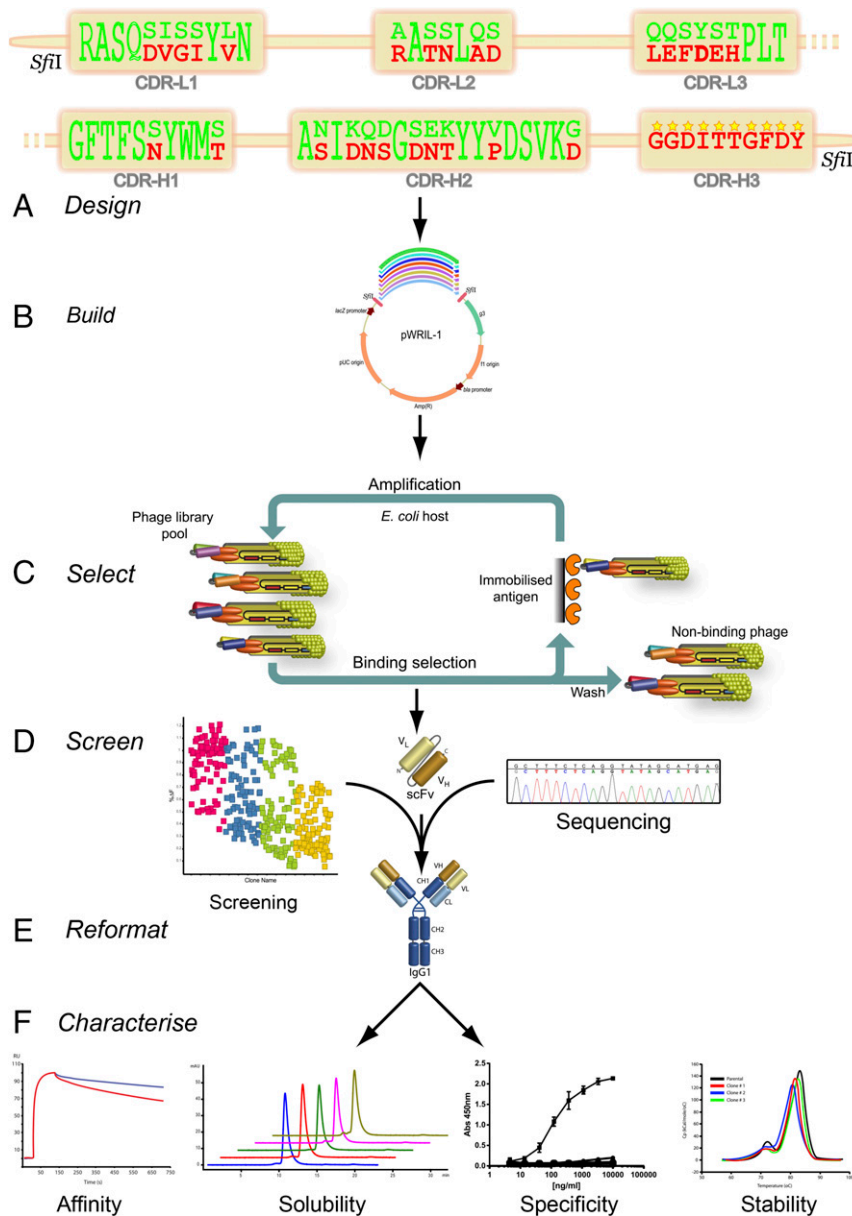


Fig. 1. Schematic of ABS library design, selection and screening principles. (A) Amino acid sequences are shown for the v-domains of Par-RAGE and destination germ-line (DPK9-DP54) scFvs in V_L-V_H format. Rat parental antibody-specific residues are highlighted in red, and human germ-line-matching residues are highlighted in green. At each position where the rat and human residues differed, both residues were encoded for in the ABS-RAGE library. This principle was applied to all CDRs other than the CDR-H3, in a single combinatorial library. In the CDR-H3, point mutations were permitted at a frequency of 1 ± 1 per clone. (B and C) Phage libraries were generated (B) and used in selections on cognate antigen (C). (D) Selection output clones were subsequently screened by ELISA, HTRF, and DNA sequencing to identify hits with maintained target binding and epitope specificity. (E and F) Top clones were expressed and purified as IgGs (E), before characterization of affinity by Biacore, solubility and aggregation analyses by SEC, in vitro specificity by ELISA and Biacore, and thermal stability analysis by DSC (F).

of the back mutation found in the VL FW2 of CL-Hum-RAGE not only aided stabilization of the v-domains (Fig. S74), but also removed a predicted T-cell epitope (Fig. S9). Analysis of the sequence of C21-ABS-pTau and C6-ABS-A33 showed that the ABS-derived germ-lining at key positions in multiple CDRs had ablated foreign T-cell epitopes including some that had been introduced by CDR-grafting. However, some potential foreign epitopes were still present, even after ultrahumanization (Fig. S9). This finding reflects the need to retain certain key contact residues in the paratope and balance target recognition with T-cell epitopes and overall “humanness.” The L46T back mutation in C21-ABS-pTau was not predicted to introduce a T-cell epitope and this clone retained only a single predicted foreign T-cell epitope.

It has previously been argued that another major determinant of antibody immunogenicity is likely to be the amount of non-germ-line surface residue exposure found on the v-domains (45). To assess non-germ-line surface availability, nonhuman solvent-accessible surface area (nhSASA, measured in Å²) was calculated for the parental, graft and ABS lead clones. All ABS leads demonstrated minimized nhSASA (Fig. S8B). Notably, C7-ABS-RAGE exhibited a nhSASA of 1,077.6 Å², in comparison with the Par-RAGE and Graft-RAGE at 3,084.8 and 1,957.6, respectively, which represents a 45% reduction even in comparison with the Graft-RAGE, where the CDRs are the only source of non-germ-line surface residues.

Further analyses were performed using publically available software to numerically define the human repertoire similarity of

the parental and ABS-derived leads, in comparison with 31 antibodies currently approved as therapeutics with murine, humanized or fully human v-domains. These analyses showed that the ABS clones had distinctly improved T20 (46), G (47), and Z (48) scores over parental clones. Indeed, ABS lead clones had scores placing generally in the range of values found for the fully human antibody group (Fig. S8C).

Essential Non-Germ-Line CDR Content Definition via Mutational Tolerance and Structural Analyses. The screening of output clones from the ABS-pTau library identified 188 sequence-unique hits with binding signals \geq the parental scFv (Fig. S3A). For residues targeted in the library for binary substitution, positional amino acid retention frequencies were calculated for these hits and expressed as a percentage (Fig. S10 A and B). Amino acid positions with parental residue retention frequencies of $>75\%$ were labeled “strongly maintained” (SM), i.e., with the chicken residue being positively selected. Those with frequencies below 25% were labeled “strongly deleted” (SD), i.e., the human germ-line residue being preferred.

When the SM residues were compared with those previously predicted to be key contacts via a cocrystal structure (3), the two populations were found to clearly overlap. Across both chains, however, SM positions were found to be only 29.6% (17 of 55) of the total CDR residues outside the CDR-H3. In the V_H domain, Q33, T52, S53, R54 were all predicted contact residues and all were SM, with retention frequencies $>90\%$. G55 and G56 were also predicted to be key contacts but were not sampled in the library, as they were fully conserved human to chicken. Interestingly, the S53G substitution, although not heavily favored in the selected population, could clearly be functional, as seen in the C21-ABS-pTau clone, so long as T52, R54, G55, and G56 were maintained (Fig. S4). Other SM residues in the V_H were found to be contact-proximal and/or potentially critical for appropriate presentation of the contact residues, such as M35, A49, G50, V57, and G59. Of four predicted contact residues in the V_L (3), only Y91 was found to be SM and was retained at 100%. Other SM residues were predominantly found in stem-loop positions of CDR-L3 (G89, G96, G98) and CDR-L1 (G34), which may be influential on loop structure (35). Additionally, the SM N51 site forms structurally supportive hydrogen bonds between the CDR-L1 and V_L FW2 (3).

Out of 33 residues sampled by binary substitution, only a single SD residue (V_H L29) was identified, suggesting that all 16 other non-SM residues were interchangeable. On the basis of these analyses, we identified the “essential non-germ-line CDR content,” meaning those essential parental residues that cannot be germ-lined, even if compensated by the mutation of a residue elsewhere in the paratope (Fig. 2 A–C). These findings also informed the minimization of chicken residue content by making a combination clone, Combo-ABS-pTau. This clone contains the most “human” variant of each CDR that had been observed in the top ABS-pTau hits (Fig. S4 and Table S1). This reduced non-germ-line content by another 6 residues versus C21-ABS-pTau, pushing the Combo-ABS-pTau to 76% human in the CDRs, but adding one more predicted T-cell epitope than C21-ABS-pTau (Fig. S9). The retained non-germ-line residues in Combo-ABS-pTau closely matched to the SM set of residues described above (Fig. S10 A and B). Combo-ABS-pTau was found to be soluble, stable and maintained the binding affinity and specificity of Par-pTau (Table S1 and Fig. S7B).

Similar data to that described above was found for ABS-A33 (Fig. S10 C and D). Furthermore, the combined analyses of retention frequencies in 5 separate ABS humanizations showed that some CDR loop regions known to have low potential to form contacts with antigen (32) were highly amenable to humanization. Residues 60–65 of the VH -CDR2, 24–27 of the VL -CDR1 in kappa and lambda chains, 89, 93, and 97 of the VK -CDR3 and multiple VL -CDR2 positions could frequently be germ-lined

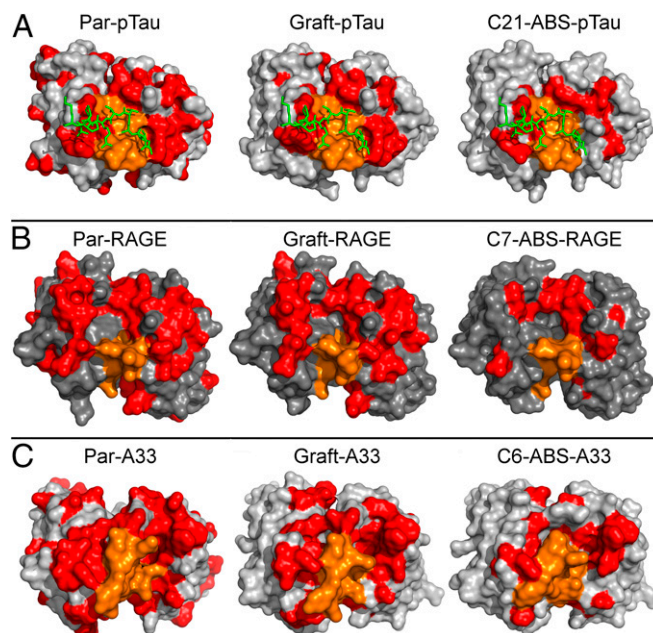


Fig. 2. CDR germ-lining illustration via surface space-fill plots of non-germ-line amino acid retention. (A) Heatmap (based on cocrystal structure PDB 4GLR) of non-germ-line residue content in the anti-pTau binding site for Par-pTau, Graft-pTau and C21-ABS-pTau. Residues matching human DP47/DPL16 germ lines are shown (spacefill) in gray, non-germ-line residues in orange (CDR-H3) or red (all other CDRs). The target pTau phospho peptide is included in green, illustrating the predominant retention of surface-exposed residues involved in the functional paratope in clone C21-ABS-pTau. Although cocrystal structures for anti-RAGE (B) and anti-A33 (C) were not available, structural modeling showed that the ABS process clearly defines residues that may be essential for antigen-binding function.

(Fig. S11 A–C). In the majority of positions sampled, however, no retention frequencies were observed that might allow prediction of humanization success a priori. Germ-lining of positions was not exclusively observed at positions where the amino acids were homologous, as also demonstrated in Table S1.

Discussion

Despite considerable investigation, current antibody humanization methods often create therapeutic molecules with significant risk factors for the failure of a lead drug due to potential immunogenicity and/or poor pK in the clinic (6) or because the molecule cannot be manufactured and delivered in a cost-effective manner (49). These risks are potentially exacerbated if the lead is derived from hosts such as rats, rabbits, or chickens, rather than the heavily characterized antibody repertoires of mice and humans.

Antibodies from alternative immune species can provide excellent IgGs with unique functional characteristics against problematic targets (e.g., highly conserved across species), but their antibodies are also known to exhibit unique sequence/structural features (19). These antibodies require maximal humanization and development validation if they are to gain broad acceptance as potential clinical leads. Indeed, despite their therapeutic potential, there are currently no chicken antibodies and only one known humanized rabbit antibody in the clinic (50). In establishing the ABS technology we have shown that it is possible to minimize clinical and manufacturing concerns, by making antibodies from all three sources with excellent drug-like properties: highly expressed, biophysically stable, soluble, and of low immunogenicity risk.

When analyzed in silico, human identity and T-cell epitope risk appeared to be indivisible between C7-ABS-RAGE and

currently marketed fully human antibodies, with C21-ABS-pTau and C6-ABS-A33 comparable to the best of the humanized mouse antibodies currently approved for clinical use. This finding is of key importance as it shows that the ABS process intrinsically minimizes the number of non-germ-line residues in the v-domains, reducing the potential for HLA class II peptide content that could drive the CD4+ T-cell help that is believed to be a key component of class-switched, high-affinity, anti-drug IgG responses (5).

The drive toward germ-line content in v-domains is underpinned by core theories of self-tolerance: Thymic tolerance in any given individual that defines “self” is dominated by the deletion of T cells recognizing self-antigens (5). Although individual antibody v-domain sequences often accrue significant deviations from germ line in the CDRs due to somatic hypermutation, those individual unique sequences are only likely to be tolerated in the individual which made the original B cell. The base set of 9-mer peptides that are common to, and likely to be tolerated by, all humans (excepting for allotypic differences), is therefore encoded for by the germ-line v-domain sequences that are expressed at high levels across many individuals (51). Importantly, this theory has been experimentally tested in mice, where CD4+ T cells in adult animals are unresponsive to mouse germ-line v-domains (51). It should be noted, however, that analysis of the predictive power of *in silico* T-cell epitope prediction has questioned its accuracy. This potential inaccuracy may be due to the observation that current prediction software is accurate at predicting the dominant DR-displayed peptides, but lacks accuracy in predicting DP and/or DQ alleles (52). These findings further support the rationale to drive the full v-domain sequence (inclusive of CDRs) as close as possible to human germ line, due to our inability to fully avoid false negatives in *in silico* epitope screening. Predictive power of immunogenicity analyses post-ABS could also be improved by performing *in vitro* antigen stimulation assays (52).

The use of preferred human germ-line frameworks is a critical element of the ABS technology, as this gives great confidence in the stability and solubility qualities of the resulting ultra-humanized lead antibodies. Other humanization methods do not factor in the CDRs themselves as mediators of stability and solubility, in addition to the frameworks. Antibodies from species with limited starting framework diversity in both the V_H and V_L genes fit the ABS technology particularly well. Indeed, chickens and rabbits use V_H repertoires that are highly homologous to human V_H3 domain (19). For murine antibodies, FW diversity in the functional repertoire is much higher than for chickens or rabbits (19). Prior estimations of v-domain homology, pairing angle, and V_H - V_L packing are therefore prudent to predict whether preferred germ lines other than DP54 and DPK9 should be used during ABS of murine clones (13). Additionally, so-called fully human antibody sequences derived from naïve phage display libraries, human B-cell cloning, or transgenic animals will also typically have unnecessary deviations from germ line, caused by somatic hypermutation (1). The ABS process may also be applicable in rapidly germ-lining these antibodies before clinical use.

Although it has previously been shown that some redundant CDR residues can be germ-lined via iterative testing of point mutations (5, 15) or *in silico* modeling (14), neither of these methods has the power to simultaneously sample e.g., $>2^{30}$, concurrent, potentially synergistic, substitutions that are distal in sequence space, while intrinsically selecting for function. Additionally, methods that maintain the animal CDR-H3 (+/- CDR-L3), then

sample human repertoire diversity to return binding affinity (21, 53), may suffer from an inability to recapitulate the critical structural characteristics found outside the CDR-H3s of non-murine antibodies, as exemplified by our anti-pTau mAb (3). These methods also frequently leave, or generate, significant numbers of framework mutations away from germ line, which can lower the stability of v-domains (22). Indeed, the C7-ABS-RAGE clone illustrated that the CDRs from XT-M4 could be heavily germ-lined and the back mutations from classical humanization fully removed, greatly improving stability in the final molecule.

This study illustrates that three separate antibodies from three species, targeting three different epitopes, all have high levels of sequence tolerance in their paratopes that can be exploited for v-domain risk reduction engineering without the need for prior structural analyses. The retention of SM residues in the CDRs of selected clones after ABS strongly correlated with the prediction of key contact residues in the cocrystal structure of anti-pTau with its target antigen. Residues were also found to be SM if they were likely to be critical in the correct presentation of CDR loops. In only one case was a framework back mutation necessary to include during humanization (V_L L46T, anti-pTau). Interestingly, a classical humanization study performed very recently (by another group) on the anti-pTau antibody also sampled the L46 position and found it to be a necessary back mutation to humanize this antibody (54). Importantly, however, four other back mutations in multiple FW regions were also found to be necessary. In the current study we show that the ABS process ameliorates the need for those back mutations to return full binding affinity. This observation suggests that many of the back mutations required during classical humanization of anti-pTau, anti-RAGE, and anti-A33 were likely necessitated by the retention of non-germ-line CDR residues that clash with human framework residue side chains, but are functionally redundant in antigen binding. Importantly, this study therefore suggests that the loss of function in our grafted clones was not due to an inherent defect in V_H / V_L packing, with the exception of the need for L46T in ABS-pTau clones. Rather, mutations in the CDRs that lead to “local accommodation” improvements are sufficient to recover affinity.

ABS intrinsically minimized redundant animal-derived CDR content by selecting for the retention of essential non-germ-line residues and allowing the rest of the CDR to be converted to the sequence of the destination v-gene. This approach thereby simultaneously optimized all functional parameters of these three potential therapeutic antibodies, which were derived from species often used in monoclonal antibody generation against challenging therapeutic targets.

Materials and Methods

Based on scFv constructs, ABS libraries were synthesized and subjected to phage display selections on their cognate targets. Lead clones identified through sequence analyses and parental IgG competition assays were reformatted to IgG, expressed, purified and their function, structure, and biophysical characteristics were examined as outlined in *SI Materials and Methods*.

ACKNOWLEDGMENTS. We thank the Pfizer Post-Doctoral Research program, Will Somers, Eric Bennett, and Davinder Gill for their support and insightful commentary.

1. Nelson AL, Dhimolea E, Reichert JM (2010) Development trends for human monoclonal antibody therapeutics. *Nat Rev Drug Discov* 9(10):767–774.
2. Rader C, et al. (2000) The rabbit antibody repertoire as a novel source for the generation of therapeutic human antibodies. *J Biol Chem* 275(18):13668–13676.
3. Shih HH, et al. (2012) An ultra-specific avian antibody to phosphorylated tau protein reveals a unique mechanism for phosphoepitope recognition. *J Biol Chem* 287(53):44425–44434.
4. Miller RA, Oseroff AR, Stratte PT, Levy R (1983) Monoclonal antibody therapeutic trials in seven patients with T-cell lymphoma. *Blood* 62(5):988–995.

5. Harding FA, Stickler MM, Razo J, DuBridge RB (2010) The immunogenicity of humanized and fully human antibodies: Residual immunogenicity resides in the CDR regions. *MAbs* 2(3):256–265.
6. Jawa V, et al. (2013) T-cell dependent immunogenicity of protein therapeutics: Pre-clinical assessment and mitigation. *Clin Immunol* 149(3):534–555.
7. Jones PT, Dear PH, Foote J, Neuberger MS, Winter G (1986) Replacing the complementarity-determining regions in a human antibody with those from a mouse. *Nature* 321(6069):522–525.

8. Almagro JC, Fransson J (2008) Humanization of antibodies. *Front Biosci* 13:1619–1633.
9. Hwang WY, Foote J (2005) Immunogenicity of engineered antibodies. *Methods* 36(1):3–10.
10. Baca M, Presta LG, O'Connor SJ, Wells JA (1997) Antibody humanization using monovalent phage display. *J Biol Chem* 272(16):10678–10684.
11. Dall'Acqua WF, et al. (2005) Antibody humanization by framework shuffling. *Methods* 36(1):43–60.
12. Dennis MS (2010) CDR repair: A novel approach to antibody humanization. *Current Trends in Monoclonal Antibody Development and Manufacturing* 1(1):9–28.
13. Fransson J, et al. (2010) Human framework adaptation of a mouse anti-human IL-13 antibody. *J Mol Biol* 398(2):214–231.
14. Hanf KJ, et al. (2014) Antibody humanization by redesign of complementarity-determining region residues proximate to the acceptor framework. *Methods* 65(1):68–76.
15. Lazar GA, Desjarlais JR, Jacinto J, Karki S, Hammond PW (2007) A molecular immunology approach to antibody humanization and functional optimization. *Mol Immunol* 44(8):1986–1998.
16. Tan P, et al. (2002) "Superhumanized" antibodies: Reduction of immunogenic potential by complementarity-determining region grafting with human germline sequences: Application to an anti-CD28. *J Immunol* 169(2):1119–1125.
17. Padlan EA (1991) A possible procedure for reducing the immunogenicity of antibody variable domains while preserving their ligand-binding properties. *Mol Immunol* 28(4-5):489–498.
18. Haidar JN, et al. (2012) A universal combinatorial design of antibody framework to graft distinct CDR sequences: A bioinformatics approach. *Proteins* 80(3):896–912.
19. Finlay WJ, Almagro JC (2012) Natural and man-made V-gene repertoires for antibody discovery. *Front Immunol* 3:342.
20. Almagro JC, et al. (2014) Second antibody modeling assessment (AMA-II). *Proteins* 82(8):1553–1562.
21. Bowers PM, et al. (2013) Humanization of antibodies using heavy chain complementarity-determining region 3 grafting coupled with in vitro somatic hypermutation. *J Biol Chem* 288(11):7688–7696.
22. Sun SB, et al. (2013) Mutational analysis of 48G7 reveals that somatic hypermutation affects both antibody stability and binding affinity. *J Am Chem Soc* 135(27):9980–9983.
23. Bumbaca D, et al. (2011) Highly specific off-target binding identified and eliminated during the humanization of an antibody against FGF receptor 4. *MAbs* 3(4):376–386.
24. van Meer PJ, et al. (2013) Immunogenicity of mAbs in non-human primates during nonclinical safety assessment. *MAbs* 5(5):810–816.
25. van Aerts LA, De Smet K, Reichmann G, van der Laan JW, Schneider CK (2014) Biosimilars entering the clinic without animal studies. A paradigm shift in the European Union. *MAbs* 6(5):1155–1162.
26. Rosenberg AS (2006) Effects of protein aggregates: An immunologic perspective. *AAAPS J* 8(3):E501–E507.
27. Ahmadi M, et al. (2015) Small amounts of sub-visible aggregates enhance the immunogenic potential of monoclonal antibody therapeutics. *Pharm Res* 32(4):1383–1394.
28. Finlay WJ, et al. (2009) Affinity maturation of a humanized rat antibody for anti-RAGE therapy: Comprehensive mutagenesis reveals a high level of mutational plasticity both inside and outside the complementarity-determining regions. *J Mol Biol* 388(3):541–558.
29. Bennett MJ, et al. (2010) Engineering fully human monoclonal antibodies from murine variable regions. *J Mol Biol* 396(5):1474–1490.
30. MacCallum RM, Martin AC, Thornton JM (1996) Antibody-antigen interactions: Contact analysis and binding site topography. *J Mol Biol* 262(5):732–745.
31. Almagro JC (2004) Identification of differences in the specificity-determining residues of antibodies that recognize antigens of different size: Implications for the rational design of antibody repertoires. *J Mol Recognit* 17(2):132–143.
32. Raghunathan G, Smart J, Williams J, Almagro JC (2012) Antigen-binding site anatomy and somatic mutations in antibodies that recognize different types of antigens. *J Mol Recognit* 25(3):103–113.
33. Vajdos FF, et al. (2002) Comprehensive functional maps of the antigen-binding site of an anti-ErbB2 antibody obtained with shotgun scanning mutagenesis. *J Mol Biol* 320(2):415–428.
34. Bostrom J, et al. (2009) Variants of the antibody herceptin that interact with HER2 and VEGF at the antigen binding site. *Science* 323(5921):1610–1614.
35. Chailyan A, Marcatili P, Cirillo D, Tramontano A (2011) Structural repertoire of immunoglobulin λ light chains. *Proteins* 79(5):1513–1524.
36. North B, Lehmann A, Dunbrack RL, Jr (2011) A new clustering of antibody CDR loop conformations. *J Mol Biol* 406(2):228–256.
37. Chothia C, Lesk AM (1987) Canonical structures for the hypervariable regions of immunoglobulins. *J Mol Biol* 196(4):901–917.
38. Martin AC, Thornton JM (1996) Structural families in loops of homologous proteins: Automatic classification, modelling and application to antibodies. *J Mol Biol* 263(5):800–815.
39. Hötzel I, et al. (2012) A strategy for risk mitigation of antibodies with fast clearance. *MAbs* 4(6):753–760.
40. Vugmeyster Y, et al. (2010) Correlation of pharmacodynamic activity, pharmacokinetics, and anti-product antibody responses to anti-IL-21R antibody therapeutics following IV administration to cynomolgus monkeys. *J Transl Med* 8:41.
41. Sampei Z, et al. (2013) Identification and multidimensional optimization of an asymmetric bispecific IgG antibody mimicking the function of factor VIII cofactor activity. *PLoS One* 8(2):e57479.
42. Li B, et al. (2014) Framework selection can influence pharmacokinetics of a humanized therapeutic antibody through differences in molecule charge. *MAbs* 6(5):1255–1264.
43. Wu H, et al. (2005) Ultra-potent antibodies against respiratory syncytial virus: Effects of binding kinetics and binding valence on viral neutralization. *J Mol Biol* 350(1):126–144.
44. USFDA (2014) Guidance for Industry - Immunogenicity Assessment for Therapeutic Protein Products. Available at www.fda.gov/downloads/drugs/guidancecomplianceregulatoryinformation/guidances/ucm338856.pdf.
45. Roguska MA, et al. (1994) Humanization of murine monoclonal antibodies through variable domain resurfacing. *Proc Natl Acad Sci USA* 91(3):969–973.
46. Gao SH, Huang K, Tu H, Adler AS (2013) Monoclonal antibody humanness score and its applications. *BMC Biotechnol* 13:55.
47. Thullier P, Huish O, Pelat T, Martin AC (2010) The humanness of macaque antibody sequences. *J Mol Biol* 396(5):1439–1450.
48. Abhinandan KR, Martin AC (2007) Analyzing the "degree of humanness" of antibody sequences. *J Mol Biol* 369(3):852–862.
49. Yang X, et al. (2013) Developability studies before initiation of process development: Improving manufacturability of monoclonal antibodies. *MAbs* 5(5):787–794.
50. Strohl WR (2014) Modern therapeutic antibody drug discovery technologies. *Curr Drug Discov Technol* 11(1):1–2.
51. Bogen B, Ruffini P (2009) Review: To what extent are T cells tolerant to immunoglobulin variable regions? *Scand J Immunol* 70(6):526–530.
52. Mazor R, Tai CH, Lee B, Pastan I (2015) Poor correlation between T-cell activation assays and HLA-DR binding prediction algorithms in an immunogenic fragment of Pseudomonas exotoxin A. *J Immunol Methods* 425:10–20.
53. Rader C, Cheresch DA, Barbas CF, 3rd (1998) A phage display approach for rapid antibody humanization: Designed combinatorial V gene libraries. *Proc Natl Acad Sci USA* 95(15):8910–8915.
54. Baek DS, Kim YS (2015) Humanization of a phosphothreonine peptide-specific chicken antibody by combinatorial library optimization of the phosphopeptide-binding motif. *Biochem Biophys Res Commun* 463(3):414–420.
55. King AC, et al. (2011) High-throughput measurement, correlation analysis, and machine-learning predictions for pH and thermal stabilities of Pfizer-generated antibodies. *Protein Sci* 20(9):1546–1557.
56. Ewert S, Huber T, Honegger A, Plückthun A (2003) Biophysical properties of human antibody variable domains. *J Mol Biol* 325(3):531–553.
57. Knappik A, et al. (2000) Fully synthetic human combinatorial antibody libraries (HuCAL) based on modular consensus frameworks and CDRs randomized with trinucleotides. *J Mol Biol* 296(1):57–86.
58. Mahon CM, et al. (2013) Comprehensive interrogation of a minimalist synthetic CDR-H3 library and its ability to generate antibodies with therapeutic potential. *J Mol Biol* 425(10):1712–1730.
59. Prassler J, et al. (2011) HuCAL PLATINUM, a synthetic Fab library optimized for sequence diversity and superior performance in mammalian expression systems. *J Mol Biol* 413(1):261–278.
60. Shi L, et al. (2010) De novo selection of high-affinity antibodies from synthetic fab libraries displayed on phage as pIX fusion proteins. *J Mol Biol* 397(2):385–396.
61. Tiller T, et al. (2013) A fully synthetic human Fab antibody library based on fixed VH/VL framework pairings with favorable biophysical properties. *MAbs* 5(3):445–470.
62. Mouquet H, et al. (2010) Polyreactivity increases the apparent affinity of anti-HIV antibodies by heterologation. *Nature* 467(7315):591–595.
63. Eswar N, et al. (2006) Comparative protein structure modeling using Modeller. *Curr Protocols Bioinformatics* Chapter 5:Unit 5.6.
64. Schafer JR, Jesdale BM, George JA, Koultab NM, De Groot AS (1998) Prediction of well-conserved HIV-1 ligands using a matrix-based algorithm, EpiMatrix. *Vaccine* 16(19):1880–1884.
65. Southwood S, et al. (1998) Several common HLA-DR types share largely overlapping peptide binding repertoires. *J Immunol* 160(7):3363–3373.
66. Koren E, et al. (2007) Clinical validation of the "in silico" prediction of immunogenicity of a human recombinant therapeutic protein. *Clin Immunol* 124(1):26–32.